ARTICLES

Characterization of ESR Active Species on Lithium Chloride-Modified Mesoporous Silica

Naotaka Chino,[†] Masaru Ogura,[†] Tetsuya Kodaira,[‡] Jun Izumi,[§] and Tatsuya Okubo*[,†]

Department of Chemical System Engineering, The University of Tokyo, 7-3-1 Hongo, Bunkyo-ku, Tokyo 113-8656, Japan, Nanoarchitectonics Research Center, National Institute of Advanced Industrial Science and Technology, AIST Tsukuba central 5, Tsukuba, Ibaraki 305-8565, Japan, and Kashiwa Laboratory, Institute of Research and Innovation, 1201 Takada, Kashiwa, Chiba 277-0861, Japan

Received: June 28, 2004; In Final Form: February 23, 2005

The surface of mesoporous silica with regular nanometer-sized pores and high surface area has been modified by metal ions or functional groups to introduce specific interactions. We found that ESR active species were formed on lithium chloride (LiCl)-modified mesoporous silica after heat treatment. The structure and the surface properties of LiCl-modified mesoporous silica were characterized by XRD, ESR, nitrogen adsorption, UV−vis−NIR, and TPD. The results suggest that the ESR active species were generated on the surface in response to heat treatment above 673 K. Moreover, it was found for the first time that LiCl-modified mesoporous silica after the heat treatment has reversible adsorption properties for hydrogen under room temperature and atmospheric pressure.

1. Introduction

Since the discovery of mesoporous silica in the early 1990s,[1−2] many investigations have been devoted to the discovery of new structures and the improvement of synthetic methods. These materials with regular nanometer-sized pores and high surface area have attracted a great deal of attention as new candidates for catalysis and adsorption. However, investigations of the original mesoporous silica have been limited, since the surface properties depend mainly on silanol groups. Therefore, mesoporous silica modified by metal ions or functional groups has been investigated with regard to its ability to generate specific catalytic functions or adsorption properties. The incorporation of transition metals into the silicate framework is one strategy utilized in creating active sites. Several examples of metal incorporation into mesoporous silicates have been demonstrated with metals such as Al, Ti, Ga, Mn, Cr, and Fe.[3−8] Modification of the silica surface through the introduction of functional groups is an alternative approach. For example, aminosilane-functionalized mesoporous silica has been reported to be an adsorbent for oxyanions under acidic conditions.[9] On the other hand, it has been reported that mesoporous silica shows mild acidity and a radical-like function to induce photocatalytic activities.[10−12] However, alkali metal ion species, for example, alkali halide, incorporated into or supported by mesoporous silica have scarcely been reported, since alkali metal ion species themselves have no such activity as mentioned above. Therefore, the properties and applicability of these materials have remained virtually unknown. In the present study, the structure and surface character of LiCl-modified mesoporous silica are characterized by XRD, ESR, nitrogen adsorption, UV−vis, NIR, and TPD. Moreover, it was found that LiCl-modified mesoporous silica after the heat treatment shows hydrogen adsorption capabilities under room temperature and atmospheric pressure due to the ESR active species.

2. Experimental Section

2-1. Sample Preparation. Mesoporous silica was prepared at room temperature in a highly acidic condition as reported in the previous study.[13] An aqueous solution of sodium silicate was added dropwise into a mixed aqueous solution of cetylpyridinium chloride and HCl under vigorous stirring. The surfactant/Si molar ratio was 0.12, and the pH value was less than 1 after mixing two solutions. After further stirring for 3 h at room temperature, the obtained precipitate was washed with water, dried at 383 K for 3 h, and calcined at 823 K for 6 h.

The pellet of mesoporous silica was prepared by pressing the powder at 200 kg/ cm^2 for 1 min. LiCl-modified mesoporous silica was prepared by impregnating pellets of mesoporous silica with saturated LiCl/ethanol solutions, followed by filtration and drying at 363 K in air. Finally, the heat treatment was carried out at various temperatures (473, 573, 673, or 773 K) at a heat-up rate of 4 K/min in helium flow (50 cm^3/min). Released gaseous species were analyzed by a quadrupole mass spectrometer (ANELVA M-QA100TS). Until the release of various gaseous compounds was completed, the samples had been kept at the predetermined temperature, followed by cooling to room temperature in helium flow.

2-2. Characterization. *X-ray Diffraction (XRD).* XRD measurements were carried out to assess the crystallinity of the samples. These studies were performed using an M03X-HF22 (Mac Science Co.) equipped with a Cu Kα radiation source (wavelength 1.5406 Å).

* Corresponding author. Phone: +81-3-5841-7348. Fax: +81-3-5800-3806. E-mail: okubo@chemsys.t.u-tokyo.ac.jp.
[†] The University of Tokyo.
[‡] Nanoarchitectonics Research Center, National Institute of Advanced Industrial Science and Technology.
[§] Kashiwa Laboratory, Institute of Research and Innovation.

10.1021/jp047212t CCC: $30.25
Published on Web 04/20/2005

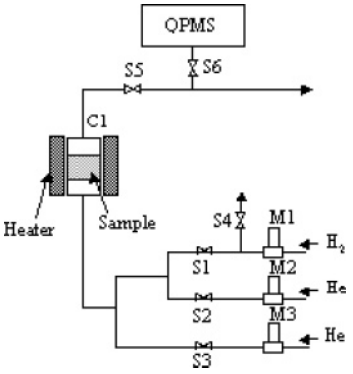

Figure 1. Schematic diagram of the apparatus. C: adsorption column, M: mass flow controller, S: solenoid valve, QPMS: quadrupole mass spectrometer.

Surface Area and Pore Size Distribution. The nitrogen adsorption measurement was performed at 77 K by using AUTOSORB-1 (Quantachrome Co.). The specific surface area of the samples was calculated from the adsorption isotherm by the Brunauer, Emmett, and Teller (BET) method. The pore size distribution of the sample was derived from nitrogen adsorption at 77 K by the Barrett, Joyner, and Halenda (BJH) method.

Fluorescent X-ray Spectroscopy (XRF). The XRF measurement was performed on a JEOL JSX-3200 for the quantitative analysis of chloride. XRF spectra were obtained at 5−30 kV and 0.0125−0.3 mA under vacuum.

ICP Emission Spectroscopy (ICP-EP). The ICP measurement was performed on an SPS3000 (SEIKO Instrument Co.) for the quantitative analysis of lithium.

Electron Spin Resonance (ESR). ESR spectra were recorded on a JEOL JES-TE200 (X-band). ESR measurements were performed at 298 K after the sample placed in a quartz tube was treated at various temperatures under vacuum and then sealed. The microwave frequency was measured as around 9.20 GHz by a frequency counter, the modulation width 0.1 and 0.5 mT, the time constant 0.1 s, and the microwave power 1.0 mW. The *g* value was estimated using a Mn^{2+} reference. Each sample was measured several times to examine the reproducibility of intensity, line widths, and *g* value.

UV−Vis−NIR Spectroscopy. UV−vis−NIR diffuse reflectance spectra of the samples were obtained with a Cary 5000 spectrometer at RT. KCl powder was used as a standard. The samples treated at various temperatures were sealed in quartz glass tubes without exposure to the air and measured. The diffuse reflection spectra were converted into absorption spectra using the Kubelka−Munk function.

Temperature-Programmed Desorption (TPD/MS). During the heat treatment, the gaseous species released from samples were analyzed by a quadrupole mass spectrometer (QPMS).

Hydrogen Adsorption/Desorption Measurement. The hydrogen adsorption/ desorption measurements were carried out in a flow-type apparatus with a fixed bed configuration, as shown in Figure 1. Adsorption and desorption runs were periodically controlled by solenoid valves (S1−4). As a pretreatment, 1.0 g of the sample was placed in a stainless steel column (C1, 10-mm inner diameter and 22-cm length) and heated just before the adsorption run at the predetermined temperature for 3 h under a helium stream (50 cm^3/min). During the adsorption run, pure hydrogen gas was fed into the column at a rate of 100 cm^3/min. After the adsorption run, pure helium was introduced at a rate of 100 cm^3/min to desorb hydrogen from the adsorbent. The temperature of the adsorbent was kept at room temperature, and each adsorption or desorption time was fixed at 10 min.

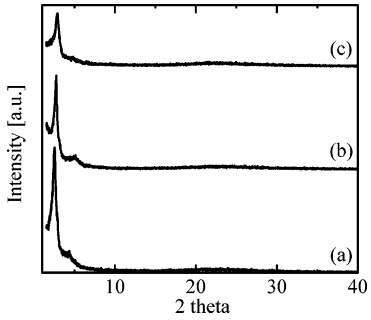

Figure 2. XRD patterns of (a) mesoporous silica, (b) LiCl-modified mesoporous silica treated at 673 K, and (c) LiCl-modified mesoporous silica treated at 773 K.

TABLE 1: BET Surface Area, Pore Diameter, Pore Volume, XRD d_{100} d-spacing, Hexagonal Unit Cell Parameter, and Pore Wall Thickness of Samples: (a) Mesoporous Silica, (b) LiCl-Modified Mesoporous Silica Treated at 673 K, and (c) LiCl-Modified Mesoporous Silica Treated at 773 K

	surface area [m^2/g]	pore diameter [nm]	pore volume [cc/g]	XRD d_{100} d-spacing [nm]	unit cell parameter [nm]	pore wall thickness [nm]
(a)	1144	2.3	0.98	3.4	4.0	1.7
(b)	1098	2.1	0.83	3.2	3.8	1.7
(c)	1010	2.0	0.64	3.1	3.6	1.6

The effluent concentration and the composition were continuously monitored by an on-line QPMS, as shown in Figure 1. The amount of adsorbed hydrogen was calculated on the basis of the difference in elution curves between samples and the α-Al_2O_3 used as a reference.

3. Results and Discussion

3-1. Characterization of Samples. As shown in Figure 2a, the XRD pattern of the original mesoporous silica sample exhibited two diffraction peaks in the low-angle region, indicating that this material has a mesopore-hexagonal regularity with an amorphous silica wall. The N_2 adsorption isotherm of mesoporous silica, which is classified as type IV of IUPAC, revealed the presence of mesopores. The structural parameters of the mesoporous silica sample derived from N_2 adsorption isotherm and powder XRD pattern are listed in Table 1. The mesoporous silica sample has a sharp pore size distribution centered at 2.3 nm and a large surface area of 1144 m^2/g.

The XRD patterns of LiCl-modified mesoporous silica treated at 673 and 773 K are shown in Figure 2, parts b and c, respectively. The patterns are almost identical to that of mesoporous silica itself. The intensity of the peaks was decreased with heat treatment temperatures. The diffraction derived from a LiCl crystal was not observed in the high-angle region, indicating that LiCl was well-dispersed on the surface of the mesoporous silica. Table 1 shows the structural parameters of LiCl-modified mesoporous silica after the heat treatment at 673 or 773 K. The pore size and the unit cell parameter decreased after the impregnation of mesoporous silica with LiCl/ethanol solutions followed by the heat treatment. The surface area and pore volume also decreased. On the other hand, the pore wall thickness was almost unchanged. These results suggest that the mesopore structure shrank as a result of the heat treatment.

3-2. Generation of ESR Active Species. Figure 3 shows the ESR spectra of mesoporous silica, LiCl crystals, and LiCl-modified mesoporous silica after heat treatment at 673 K. No ESR signal was detected on mesoporous silica, even after heat

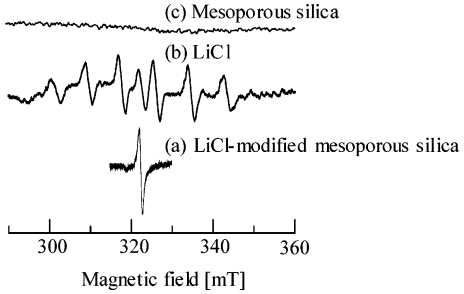

Figure 3. ESR spectra of (a) LiCl-modified mesoporous silica, (b) LiCl crystals, and (c) mesoporous silica after heat treatment at 673 K.

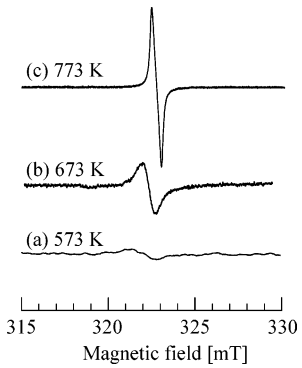

Figure 4. ESR spectra of LiCl-modified mesoporous silica at various heating temperatures; (a) 573 K, (b) 673 K, and (c) 773 K.

treatment at 673 K, because of very few defects on the silica. The ESR spectrum of the LiCl crystals after heat treatment at 673 K exhibited a central signal and 6 lines of a hyperfine structure due to the hyperfine interaction between unpaired electrons and neighboring ^{7}Li nuclei or ^{35}Cl nuclei. Such ESR active species were produced on the surface during the heat treatment because no ESR signal was observed on LiCl crystal samples before the heat treatment. The ESR spectrum of LiCl-modified mesoporous silica exhibited a sharp central signal without the hyperfine structure, which is totally different from that of LiCl crystal samples.

Figure 4 shows the ESR spectra of LiCl-modified mesoporous silica after the heat treatment at various temperatures. A sharp central signal was observed for LiCl-modified samples after heat treatment above 573 K, indicating that the ESR active species with unpaired electrons were produced by the heat treatment. The intensity of the signal was increased with increases in the heat treatment temperature. The line shape of the signal was identified as the Lorentzian one, suggesting that any unresolved hyperfine structure is much smaller than the apparent line shape. It is well-known that the ESR signal of defects on mesoporous silica has an anisotropy of the g value: ≡Si−O• (g1 = 2.0010, g2 = 2.0095, g3 = 2.078) and ≡Si• (g1 = 2.001, g2 = 2.002).[14] Because this signal was without an anisotropy of the g value, it is concluded that the ESR active species are not caused merely by defects on the silica surface but by LiCl on the silica surface (See Figure 3 also).

Figure 5 shows the relationship between the heat-treatment temperature and the g values or the line widths of peak-to-peak (ΔH_{pp}). The g values (2.004−2.007) are hardly changed by the heat treatment. On the other hand, ΔH_{pp} was simultaneously decreased from 1.5 to 0.47 mT with the heat treatment temperature. It can be considered that the change in environment around unpaired electrons results in the narrowing of ΔH_{pp}. These results show that the state of the ESR active species was changed by the heat treatment.

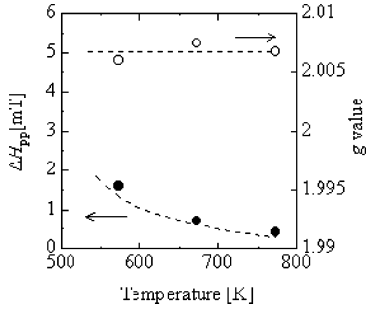

Figure 5. The heating temperature dependence of ΔH_{pp} and the g value of the LiCl-modified mesoporous silica.

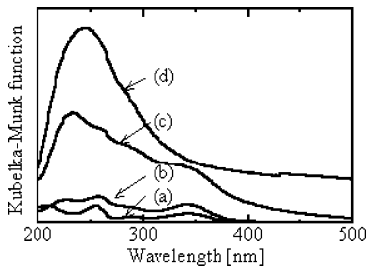

Figure 6. UV−vis absorption spectra of LiCl-modified mesoporous silica at various heating temperatures; (a) 473 K, (b) 573 K, (c) 673 K, and (d) 773 K.

3-3. Electronic Structure of ESR Active Species. UV−vis measurements were performed to investigate the electronic structure of the ESR active species. Figure 6 shows the UV−vis absorption spectra of LiCl-modified mesoporous silica at various heat treatment temperatures.

Although the absorption bands of LiCl and silica are below 200 nm,[12,15] all spectra show complex bands in the UV region. The detection of absorption bands in samples provides evidence for the presence of an unusual electronic structure including the sites trapping unpaired electrons or holes. It is indicated that ESR active species have the trap-sites of unpaired electrons and holes. A great deal of research has been devoted to interpreting the absorption bands of trap-sites generated by the irradiation in ionic crystals (LiF,[16] LiCl,[17] Li_2O,[18] and $LiAlO_2$[19]). On the basis of the analogy with such ionic crystals, it is not easy to propose a possible trap-site type corresponding to these bands, since the ESR active species on LiCl-modified mesoporous silica are merely generated by the heat treatment.

After the heat treatment at higher temperatures, the intensity of the absorption bands increased, as was observed in the ESR signal, and the line shape of the bands changed. After the heat treatment above 673 K, an absorption band appeared in the visible region and the sample color changed from white to gray-black. The appearance of absorption in the visible region corresponds to this color change. The complex bands in the UV−vis region indicate the presence of various active sites including unpaired electrons or holes on the surface of silica/LiCl. As mentioned above, it cannot be determined which band structure represents an unpaired electron, as shown in the ESR signal. The narrowing of the ESR signal corresponds to the increase in band intensity and the appearance of a band tail in the visible region. It is therefore indicated that an increase in the number of unpaired electrons in a similar environment or an enhancement of the mobility of unpaired electrons by spreading of the trap-site induces narrowing of the ESR signal.

Figure 7 shows UV−vis absorption spectra of LiCl and mesoporous silica after heat treatment at 673 K. Both spectra showed less absorption in the UV region compared with that of LiCl-modified mesoporous silica after heat treatment at

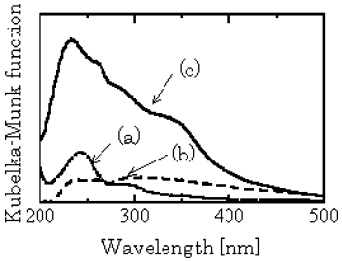

Figure 7. UV−vis absorption spectra of (a) mesoporous silica, (b) LiCl, and (c) LiCl-modified mesoporous silica after heat treatment at 673 K.

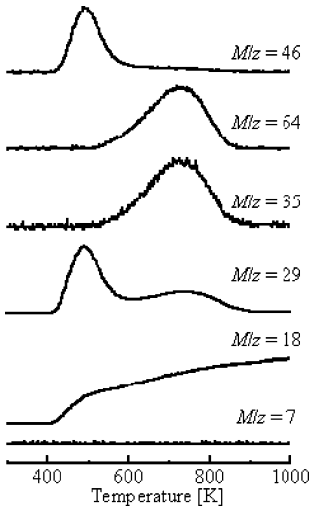

Figure 8. MS profiles of the gaseous compounds produced during the heat treatment.

673 K. These results indicate that a few defects in mesoporous silica are produced by the heat treatment (Figure 7a). LiCl-modified mesoporous silica exhibited stronger absorption in all regions, supporting the proposal that LiCl-modified mesoporous silica has more ESR active species than LiCl or mesoporous silica.

3-4. Surface Change during Heat Treatment. *TPD/MS Measurement.* The above experiments indicate that the ESR active species are produced during the heat treatment. Temperature-programmed desorption (TPD) was performed to investigate the gaseous compounds released from as-prepared LiCl-modified mesoporous silica at elevated temperatures. Figure 8 shows the profiles of mass spectra of the gaseous compounds released during the heat treatment. Adsorbed water ($M/z = 18$) and ethanol ($M/z = 46$) were desorbed below 473 K. Successively, ethyl chloride ($M/z = 64$) was released above 473 K instead of ethanol as indicated by the detection of $M/z = 64$ (CH_3CH_2Cl) and $M/z = 35$ (Cl). Two peaks of $M/z = 29$ (CH_3CH_2) correspond to the desorption of ethanol below 473 K and the release of ethyl chloride above 473 K, respectively. On the other hand, lithium ($M/z = 7$) could not be detected at all the temperatures. In the case of LiCl bulk samples with ethanol, water and ethanol were released at all temperatures, but chloride-containing species were not released, even below 673 K. These results suggest that LiCl dispersed on the silica is less stable and more reactive than LiCl crystal above 473 K.

Quantitative analyses of lithium and chloride by ICP-EP and XRF were performed, respectively, to determine the amount of released chloride and lithium. The amount of LiCl in the samples before the heat treatment was 5.6 wt %. Figure 9 shows the amounts of lithium and chloride released from the LiCl-modified mesoporous silica after the heat treatment at various temperatures. It was revealed that very little lithium was released from the sample. In contrast, chloride was certainly released at elevated temperatures, and the amount of released chloride was dependent on the heat treatment temperature. These findings support the TPD/MS results.

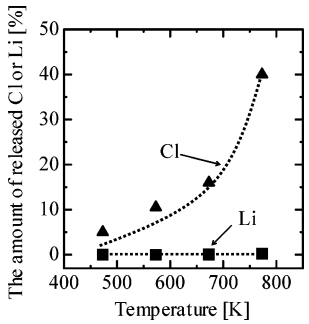

Figure 9. The heating temperature dependence of the amount of released Cl and Li.

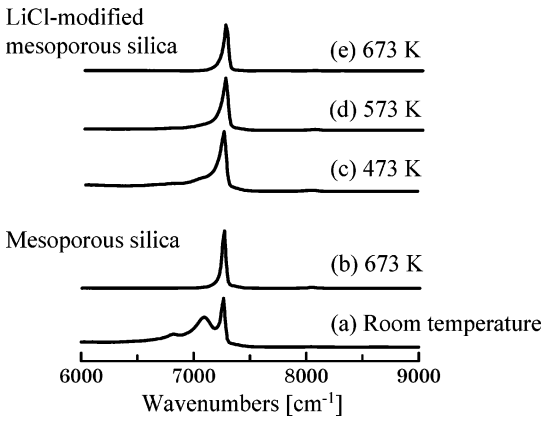

Figure 10. NIR spectra of (a,b) mesoporous silica and (c−e) LiCl-modified mesoporous silica at various heating temperatures; (a) room temperature, (b) 673 K, (c) 473 K, (d) 573 K, and (e) 673 K.

NIR Spectra. NIR measurements were performed to investigate the reactivity of the silica surface. Figure 10, parts a,b and parts c−e, show NIR spectra of mesoporous silica and LiCl-modified mesoporous silica, respectively. The spectra of mesoporous silica before heat treatment showed the bands due to water adsorbed on the silica surface and silanol groups. A sharp band at 7250 cm^{-1} is assigned to the first overtone of the OH stretching fundamental of isolated silanol groups, and two bands at 7090 cm^{-1} and 6850 cm^{-1} are assigned as two overtones of stretching fundamentals of adsorbed water from the literature.[20] The first overtone of the OH stretching fundamental of hydrogen-bonded silanol groups contributes in part to the band at 7090 cm^{-1}. On the other hand, after the heat treatment at 673 K, only the band due to the isolated silanol group was detected (Figure 10b). This result indicates that adsorbed water was almost released and that hydrogen-bonded silanol groups disappeared after the heat treatment. Figure 10, parts c−e, shows NIR spectra of LiCl-modified mesoporous silica after heat treatment at various temperatures. Heat treatment at higher temperatures resulted in the decrease in the peak intensity of adsorbed water and hydrogen-bonded silanol groups. After the heat treatment at 673 K, the NIR spectrum of LiCl-modified mesoporous silica was almost the same as that of mesoporous silica, suggesting that LiCl on the silica surface hardly reacts with the silanol groups. The instability of LiCl dispersed on the silica surface causes the release of Cl, as revealed by the TPD/MS results. Such instability is considered

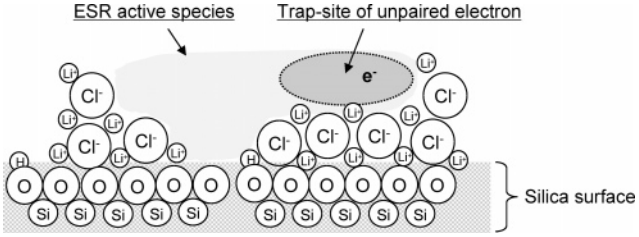

Figure 11. Schematic drawing of ESR active species.

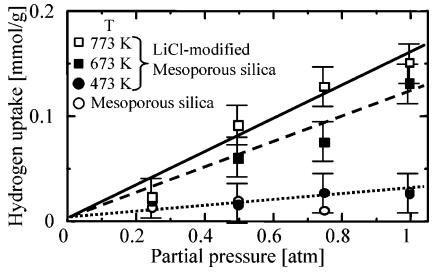

Figure 12. Hydrogen uptakes at room temperature on LiCl-modified mesoporous silica (□, ■, ●) and original mesoporous silica (○): *T*, heat treatment temperature (K).

to induce the ESR active species on the surface during the heat treatment.

3-5. ESR Active Species on the Surface. On the basis of these results, the state of ESR active species is proposed. The release of chloride shown in TPD/MS results indicates that LiCl on the surface was changed during the heat treatment. On the other hand, the silica surface was almost unchanged during the heat treatment as indicated from the ESR and NIR results. Therefore, ESR active species are generated on LiCl or near the interface between LiCl and silica surface. The sharp ESR signal indicates that unpaired electrons are trapped in sites larger than a point defect such as an F center. Moreover, the broadened UV−vis spectra suggest that ESR active species with various sizes including unpaired electrons and holes were produced on the surface, as shown in Figure 11.

3-6. Hydrogen Uptake at Room Temperature. Figure 12 shows the hydrogen uptakes of LiCl-modified mesoporous silica along with that of untreated mesoporous silica. Hydrogen uptakes of the unmodified mesoporous silica and the LiCl-modified mesoporous silica after the heat treatment at 473 K were small. In contrast, the hydrogen uptakes of LiCl-modified mesoporous silica after heat treatment at 673 or 773 K were significantly higher. The samples after the heat treatment above 673 K show reversible hydrogen adsorption. These results suggest that hydrogen-adsorption capability is generated by the heat treatment. Hydrogen uptake increased in proportion to the hydrogen concentrations. The adsorbed hydrogen was completely desorbed in 10 min, indicating that hydrogen was adsorbed on LiCl-modified samples via the weak interaction.

Because both the active sites with the ESR active species and the hydrogen adsorption capability were induced by the heat treatment and also increased simultaneously depending on the treatment temperature, it is reasonable to conclude that the ESR active species on LiCl-modified mesoporous silica could increase the hydrogen adsorption capacity. On the other hand, the ESR active species of the LiCl bulk samples have no hydrogen adsorption capability. These results suggest that the ESR active species of LiCl-modified mesoporous silica after heat treatment are more active for hydrogen molecules than those of LiCl bulk samples.

A number of studies have been carried out regarding the increase of hydrogen uptake by the modification of hydrogen adsorption sites in porous materials. For example, Forster et al. have reported that unsaturated Ni^{2+} sites in nanoporous nickel phosphate (VSB-5) strongly interact with hydrogen molecules at 77 K; VSB-5 therefore shows hydrogen physisorption properties competitive with those of zeolites and activated carbons.[21] Nishiyama et al. have reported that the number of hydrogen molecules occluded in palladium-containing NaY zeolites increases with the palladium content. The allocation of moles of hydrogen atoms to palladium gives H/Pd ratios larger than unity.[22] Metals (Ni, Pd, or Pt) forming these adsorption sites also have reversible hydrogen adsorption properties under some specific conditions. Judging from the results of LiCl without hydrogen adsorption properties at room temperature, the hydrogen adsorption site in LiCl-modified mesoporous silica is different from such adsorption sites formed by metal. On the other hand, novel hydrogen adsorption properties due to dangling bonds or defects on carbon,[23] boron nitride,[24] or carbon nitride[25] materials have been reported. These findings suggest that unstable sites in materials, such as defects, should be utilized as hydrogen adsorption sites. However, those hydrogen adsorption sites almost show irreversible hydrogen adsorption. The hydrogen adsorption site on LiCl-modified mesoporous silica is characteristic from the standpoint of the reversible hydrogen adsorption/desorption occurring at room temperature and atmospheric pressure. The electronic structure of this adsorption site may allow for an excellent strategy to achieve hydrogen adsorption under such mild conditions. Details regarding the relationship between the structure and hydrogen adsorption properties will be reported elsewhere.

4. Conclusions

It was found that the ESR active species were generated on LiCl-modified mesoporous silica after the heat treatment above 673 K. The ESR active species on LiCl-modified mesoporous silica were increased, and the state of the ESR active species was changed with the heat-treatment temperature. It was found that these phenomena corresponded well with the increase in the amount of hydrogen adsorbed reversibly. The present results suggest that ESR active species with trap-sites of unpaired electrons or holes have a significant interaction with hydrogen molecules at room temperature.

Acknowledgment. Mesoporous silica sample was synthesized by Dr. Y. Setoguchi (Joint Research Center, Nagasaki University). Mr. S. Sakae (University of Tokyo) is acknowledged for his help in XRF measurements.

References and Notes

(1) Yanagisawa, T.; Shimizu, T.; Kuroda, K.; Kato, C. *Bull. Chem. Soc. Jpn.* **1990**, *63*, 988.
(2) Kresge, C. T.; Leonowiez, M. E.; Roth, W. J.; Vartuli, J. C.; Beck, J. S. *Nature* **1992**, *395*, 710.
(3) Leroux, F.; Dewar, P. J.; Intissar, M.; Ouvrard, G.; Nazar, L. F. *J. Mater. Chem.* **2002**, *12*, 3245.
(4) Wu, P.; Iwamoto, M. *J. Chem. Soc., Faraday Trans.* **1998**, *94*, 2871.
(5) Corma, A.; Navarro, M. T.; Perez-Pariente, J. *J. Chem. Soc., Chem. Commun.* **1994**, 147.
(6) Kosslick, H.; Lischke, G.; Walther, G.; Storek, W.; Martin, A.; Fricke, R. *Microporous Mater.* **1997**, *9*, 13.
(7) Rey, F.; Shankere, G.; Mashmeyer, T.; Thomas, J. M.; Bell, R. G. *Top. Catal.* **1996**, *3*, 121.
(8) Thomas, J. M. *Faraday Discuss.* **1995**, 519.
(9) Yoshitake, H.; Yokoi, T.; Tatsumi, T. *Chem. Mater.* **2002**, *14*, 4603.
(10) Inaki, Y.; Yoshida, H.; Yoshida, T.; Hattori, T. *J. Phys. Chem. B* **2002**, *106*, 9098.

(11) Inaki, Y.; Yoshida, H.; Hattori, T. *J. Phys. Chem. B* **2002**, *104*, 10304.
(12) Yoshida, H.; Kimura, K.; Inaki, Y.; Hattori, T. *Chem. Commun.* **1997**, 129.
(13) Setoguchi, Y.; Teraoka, Y.; Moriguchi, I.; Kagawa, S.; Tomonaga, N.; Yasutake, A.; Izumi, J. *J. Porous Mater*. **1997**, *4*, 129.
(14) Skuja, L. *J. Non-Cryst. Solids* **1998**, *239*, 16.
(15) Eby, E.; Teegarden, K. J.; Dutton, D. B. *Phys. Rev*. **1959**, *116*, 5.
(16) Seifert, N.; Vijayalakshmi, S.; Yan, Q.; Allen, J. L.; Barnes, A. V.; Albridge, R. G.; Tolk, N. H. *Phys. Rev. B* **1995**, *51*, 16403.
(17) Takiyama, K. *J. Phys. Soc. Jpn.* **1978**, *44*, 1627.
(18) Uchida, K.; Noda, K.; Tanifuji, T.; Nasu, S.; Kirihara, T.; Kikuchi, A. *Phys. Status Solidi* **1980**, *58*, 557.
(19) Auvray, M. H.; Perez, A.; Dunlop, A. *Philos. Mag. B* **1988**, *57*, 137.
(20) Anderson, J. H.; Wickersheim, K. A. *Surf. Sci*. **1964**, *2*, 252.
(21) Forster, P. M.; Eckert, J.; Chang, J. S.; Park, S. E.; Ferey, G.; Cheetham, A. K. *J. Am. Chem. Soc*. **2003**, *125*, 1309.
(22) Nishiyama, N.; Kishi, T.; Mizushima, T.; Matsumoto, A.; Tsutsumi, K. *J. Alloys Compd.* **2001**, *319*, 312.
(23) Orimo, S.; Major, G.; Fukunaga, T.; Zuttel, A.; Schlapbach, L.; Fujii, H. *Appl. Phys. Lett.* **1999**, *75*, 3093.
(24) Tang, C.; Bando, Y.; Ding, X.; Qi, S.; Golberg, D. *J. Am. Chem. Soc*. **2002**, *124*, 14550.
(25) Ohkawara, Y.; Kusaka, K.; Ohshio, S.; Higa, A.; Toguchi, M.; Saitoh, H. *Jpn. Appl. Phys.* **2003**, *42*, 5251.